OXFORD

Original Manuscript

RUNX2 mutation reduces osteogenic differentiation of dental follicle cells in cleidocranial dysplasia

Yang Liu[1], Yixiang Wang[2], Xiangyu Sun[1], Xianli Zhang[1,3], Xiaozhe Wang[1], Chenying Zhang[1,*] and Shuguo Zheng[1,*]

[1]Department of Preventive Dentistry, Peking University School and Hospital of Stomatology, National Engineering Laboratory for Digital and Material Technology of Stomatology, Beijing Key Laboratory of Digital Stomatology, 22 Zhongguancun Avenue South, Haidian District, Beijing 100081, PR China, [2]Central Laboratory, Peking University School and Hospital of Stomatology, National Engineering Laboratory for Digital and Material Technology of Stomatology, Beijing Key Laboratory of Digital Stomatology, 22 Zhongguancun Avenue South, Haidian District, Beijing 100081, PR China, and [3]Department of Stomatology, Xuanwu Hospital Capital Medical University, 45 Chang Chun Street, Xicheng District, Beijing 100053, PR China

*To whom correspondence should be addressed. Tel: +86 10 82195510; Fax: +86 10 62173404; Email: zhengsg86@gmail.com (Shuguo Zheng). Tel: +86 10 82195558; Fax: +86 10 62173404; Email: zhangchy168@163.com (Chenying Zhang)

Abstract

Disturbed permanent tooth eruption is common in cleidocranial dysplasia (CCD), a skeletal disorder caused by heterozygous mutation of *RUNX2*, but the mechanism underlying is still unclear. As it is well known that dental follicle cells (DFCs) play a critical role in tooth eruption, the changed biological characteristics of DFCs might give rise to disturbance of permanent tooth eruption in CCD patients. Thus, primary DFCs from one CCD patient and normal controls were collected to investigate the effect of *RUNX2* mutation on the bone remodeling activity of DFCs and explore the mechanism of impaired permanent tooth eruption in this disease. Conservation and secondary structure analysis revealed that the *RUNX2* mutation (c.514delT, p.172fs) found in the present CCD patient was located in the highly conserved RUNT domain and converted the structure of RUNX2. After osteogenic induction, we found that the mineralised capacity of DFCs and the expression of osteoblast-related genes, including RUNX2, ALP, OSX, OCN and Col Iα1, in DFCs was severely interfered by the *RUNX2* mutation found in CCD patients. To investigate whether the osteogenic deficiency of DFCs from the CCD patient can be rescued by *RUNX2* restoration, we performed 'rescue' experiments. Surprisingly, the osteogenic deficiency and the abnormal expression of osteoblast-associated genes in DFCs from the CCD patient were almost rescued by overexpression of wild-type *RUNX2* using lentivirus. All these findings indicate that *RUNX2* mutation can reduce the osteogenic capacity of DFCs through inhibiting osteoblast-associated genes, thereby disturbing alveolar bone formation, which serves as a motive force for tooth eruption. This effect may provide valuable explanations and implications for the mechanism of delayed permanent tooth eruption in CCD patients.

Introduction

Runt-related transcription factor-2 (RUNX2) is a member of RUNX family located on chromosome 6p21 and is essential for osteoblast differentiation and skeletal morphogenesis (1,2). As a master transcriptional factor involved in bone formation, *RUNX2* is crucial for both intramembranous and endochondral ossification (3,4). *RUNX2* is continuously expressed throughout intramembranous ossification. While *RUNX2* expression is restricted to those cells

located at peripheral mesenchymal condensations during endochondral ossification (5). *RUNX2* null (*RUNX2^-/-^*) mice died just after birth and absolutely failed in bone formation, whereas the development of cartilage was nearly normal (1,6). In addition, another verified key role of *RUNX2* in osteoblast differentiation is that *RUNX2* can regulate the expression of several osteoblast marker genes, including osterix (*OSX*), osteocalcin (*OCN*), bone sialoprotein (BSP), osteopontin (OPN) and collagen I (Col I) (5,7–11).

RUNX2 mutation is responsible for cleidocranial dysplasia (CCD; MIM 119600), a rare autosomal dominant skeletal disorder (12,13). The primary clinical features of CCD are mainly manifested in the bone and teeth, including aplastic or hypoplastic clavicles, persistently open or delayed closing of fontanelle, distal phalanx dysplasia, short stature and multiple dental anomalies such as supernumerary teeth, retention of primary dentition and delayed eruption of permanent teeth (14,15). However, the phenotypic spectrum differs dramatically among CCD patients and those abnormalities are not observed in all individuals (14,16). Despite the numerous skeletal deficiencies observed in CCD individuals, the dental anomalies are usually their main complaints, especially for impaired permanent tooth eruption (17).

Tooth eruption is a fundamental developmental and physiological process, which requires both bone resorption and bone formation (18,19). During tooth eruption, bone resorption promotes the formation of tooth eruption pathway, while bone formation serves as an eruption force to propel the tooth out of its bony crypt (20). It had been widely accepted that the dental follicle, a loose connective tissue sac between the alveolar bone of the socket and the enamel organ of the unerupted tooth, is crucial for tooth eruption (21,22). The reason is that the dental follicle can regulate the required osteoclastogenesis and osteogenesis for tooth emergence (19,20). While it is noted that dental follicle cells (DFCs) are precursors of alveolar osteoblasts and can differentiate into the alveolar bone and the mineralised bone-like cementum (19,23,24). Therefore, DFCs participate in tooth eruption not only as a regulator of bone remodelling but also as the precursors of alveolar osteoblasts which are critical for bone formation during tooth eruption.

Recently, we reported a frameshift mutation of *RUNX2* in a Chinese CCD patient who is receiving treatment at our hospital for impacted permanent teeth. Our previous studies showed that this *RUNX2* mutation reduced the osteoclast-inductive capacity of DFCs and restricted the formation of tooth eruption pathway (25). However, the effect of *RUNX2* mutation on the eruption force of permanent tooth is still unknown. In this study, primary DFCs from the CCD patient and normal controls were extracted to explore the effect of *RUNX2* mutation on the osteogenic capacity of DFCs and a rescue assay was performed to verify the conclusions we got.

Materials and Methods

Participants

A 16-year-old boy, clinically and genetically diagnosed with CCD (16), and three unaffected children (aged 12–16 years) were included in the present study. This study was ethically approved by the Ethical Committee of Peking University School of Stomatology (approval No. PKUSSIRB-2012004). The methods were carried out in accordance with the relevant guidelines, including any relevant details. All the experiments in this study were carried out with informed consent.

Conservation and secondary structural analysis

Conservation analysis of the affected amino acids among nine species was performed using the Homologene database library (http://www.ncbi.nlm.nih.gov/homologene). Secondary structure of wild-type

RUNX2 (*WT-RUNX2*) and mutant *RUNX2* were predicted by PsiPred 3.3 (http://bioinf.cs.ucl.ac.uk/psipred).

Cell culture

Dental follicles were collected during exposure of impacted mandibular premolars for treatment. To obtain single DFCs suspension, dental follicles were digested in 0.3% collagenase type I (Sigma-Aldrich, MO, USA) for 40 min at 37°C. Then, the cells were cultured in a proliferation medium (PM) containing DMEM (Gibco, NY, USA), 10% fetal bovine serum (Gibco), 100 U/ml penicillin (Gibco), and 100 μg/ml streptomycin (Gibco) in an incubator at 37°C with 5% CO_2. DFCs between 3–5 passages were used in subsequent experiments.

Mutation analysis

To detect *RUNX2* status in DFCs from the CCD patient and normal control, we extracted DNA from DFCs with a General AllGen Kit (Cwbiotech, Beijing, China) according to the manufacturer's protocol. Exon 2 of *RUNX2* gene was amplified by polymerase chain reaction (PCR), and the PCR products were then sequenced with an ABI 3730 sequencer.

Immunohistochemistry

For immunohistochemistry staining, DFCs seeded on coverslips were fixed in 4% paraformaldehyde (Sigma-Aldrich) for 20 min, permeated with 0.3% Triton X-100 (Sigma-Aldrich) for 10 min, blocked in bovine serum, and incubated with primary antibodies against vimentin (Zhongshan Bioengineering Co. Ltd., Beijing, China) or cytokeratin (Zhongshan Bioengineering Co. Ltd.) at 4°C overnight. The SP immunohistochemistry kit was used with a 3, 3′-diaminobenzidine colouration kit (Zhongshan Bioengineering Co. Ltd.) according to the instruction of the manufacturer. The results were observed with a light microscope equipped with a camera (Carl Zeiss, TH, Germany).

Lentivirus construction and establishment of stably infected DFCs

The full-length human *WT-RUNX2* cDNA was subcloned with EcoR I and BamH I (NEB, MA, USA) into the pHBLV-CMVIE-ZsGreen-T2A-puro vector to generate lentivirus overexpressing *WT-RUNX2*. Lentivirus containing a green fluorescent protein (GFP) tag with no target gene was used as the negative control. The recombinant and control vectors were transfected, along with the packaging vectors psPAX2 and pMD2.G into 293T cells to produce lentivirus. The supernatant was harvested, filtered, and concentrated at 2 days post-transfection. To establish stable overexpression of human *WT-RUNX2* or negative control (GFP control) in DFCs, lentivirus (multiplicity of infection = 100) mixed with 10 ug/ml polybrene (Sigma) were used to infect the second passage of DFCs for 12 h. Then, the medium was refreshed, and DFCs were incubated for another 48 h. Infected cells were selected in the presence of 1 ug/ml puromycin (Sigma) for 7 days. Cells were observed under a fluorescent microscope to identify their infection efficiency. Real-time PCR and western blotting were used to detect the expression of *RUNX2* in surviving cells after puromycin selection.

Osteogenic differentiation

For osteogenic induction, DFCs were seeded with a density of 1×10^5 cells/well in 6-well plates. When 80% confluence was reached, the PM was changed to osteogenic medium (OM) consisting of 100 nM/l dexamethasone (Sigma-Aldrich), 10 mM/l

β-glycerophosphate (Sigma-Aldrich), and 50 μg/ml L-ascorbic acid (Sigma-Aldrich) in addition to the PM.

ALP activity test, *ALP* staining and alizarin red staining

After DFCs were cultured in PM or OM for 7 or 14 days, alkaline phosphatase (*ALP*) activity was analysed using the *ALP* Activity Assay kit (Jiancheng, Nanjing, China). Total protein was determined with the BCA method using the Pierce protein assay kit (Thermo Fisher, MA, USA). *ALP* activity relative to the control treatment was calculated after normalisation to total protein content. *ALP* staining was analysed with the *ALP* histochemical staining kit (Cwbiotech) after induction for 14 days in the OM. For alizarin red staining, after induction for 21 days in OM, DFCs were fixed with 4% paraformaldehyde and incubated with 2% alizarin red (Sigma-Aldrich) for 20 min. The image of *ALP* staining and alizarin red staining were captured by the scanner (HP, USA).

Real-time PCR

After DFCs were cultured in OM or PM for 14 days, total RNA was extracted with Trizol reagent (Invitrogen, CA, USA), and reversely transcribed into cDNA with a reverse transcription kit (Thermo Fisher). Real-time PCR was performed using the SYBR Green PCR kit (Roche Applied Science, IN, USA) on the ABI 7500 Real-Time PCR System (Applied Biosystems, CA, USA). The relative mRNA levels were normalised to the expression of GAPDH.

Western blotting analysis

After DFCs were cultured in OM or PM for 14 days, the total protein was extracted using the RIPA kit (Huaxing bio, Beijing, China). Protein concentration was tested with the Pierce protein assay kit (Thermo Fisher). The lysate was electrophoresed in 10% SDS-PAGE gels and transferred to PVDF membranes (Millipore, MA, USA). After being blocked in 5% skim milk, membranes were incubated with primary antibodies against RUNX2 (CST, MA, USA), ALP (Huaxing bio), OSX (Abcam, Cambridge, UK), Col Iα1 (Abcam) and OCN (Abcam). HRP-conjugated secondary antibody (Jackson ImmunoResearch, PA, USA) was then used. The immune-reactive bands were visualised by the enhanced chemiluminescence blotting kit (Cwbiotech). Blots against GAPDH served as a loading control.

Statistical analysis

All the experiments were repeated at least three times independently. All data was presented as the mean ± SD. Group mean values were compared, as appropriate, by Student's two-tailed t-test or one-way ANOVA with Schefe's post-hoc test. $P < 0.05$ was considered as statistically significant.

Results

Clinical manifestation of the CCD patient

This patient was a familial case, and his father was also affected. The proband showed typical CCD phenotypes, including delayed closure of sagittal suture (Figure 1A and B), hypoplastic clavicles (Figure 1C), and classic dental abnormalities. The skull anteroposterior radiographs and chest radiograph of the patient had been shown in the previous papers of our research group (16,26). Panoramic radiological and clinical examination showed that four deciduous teeth were still retained, and their successors were

impacted in the alveolar bones, though the CCD patient was already 16 years old (Figure 1D–G). In addition, nine supernumerary teeth were present in the alveolar bones (Figure 1D). Surgical exposure combined with orthodontic traction was applied on this patient and dental follicle tissues were collected during surgical exposure of the impacted canines and premolars (Figure 1H).

RUNX2 mutation analysis

Our previous study found a frameshift mutation (c.514delT, p.172fs) in the exon 2 of *RUNX2* in this patient (Figure 2A), which further confirmed the clinical diagnosis of CCD (15). Conservation analysis among nine species showed that the affected residues in RUNX2 have a high level of evolutionary conservation among different species (Figure 2B). The secondary structure analysis showed that the *RUNX2* mutation resulted in transformations of RUNX2 protein structure, and the changes were mainly located in the RUNT domain (Figure 2C). Mutation of the conserved residues and the changes of secondary structure may affect the function of the RUNX2 protein.

RUNX2 mutation reduces the expression of *RUNX2* in DFCs

The effect of this *RUNX2* mutation on the biological characterisation of DFCs was explored using primary DFCs isolated from the CCD patient (named as CCD-DFCs). Primary DFCs extracted from three gender- and age-matched normal participants were used as controls (named as CON-DFCs). Immunohistochemical staining was performed to examine the source of the cultured cells. CCD-DFCs and CON-DFCs were vimentin-positive and keratin-negative (Figure 3A), indicating that these cells were derived from mesenchymal cells. The morphology of CCD-DFCs and CON-DFCs were both similar with spindle-shaped like typical fibroblasts. The frameshift mutation of *RUNX2* (c.514delT, p.172fs) was confirmed by Sanger sequencing with DNA from CCD-DFCs (Figure 3B), which was consistent with the result using blood samples in our previous study (16). The effect of the detected *RUNX2* mutation on *RUNX2* expression was then investigated. RUNX2 mRNA level was reduced more than 50% by *RUNX2* mutation ($P < 0.05$) (Figure 3B). Western blotting result showed that RUNX2 expression at the protein level was significantly reduced by the *RUNX2* mutation (Figure 3C).

RUNX2 mutation interferes with the osteogenic ability of DFCs

DFCs are multipotent mesenchymal stem cells, which can differentiate into osteoblasts, adipocytes, chondrocytes, and neural cells under different in vitro conditions (19,23,24). In the present study, the effect of *RUNX2* mutation on the osteogenic differentiation of DFCs was explored. As *ALP* is considered to be an early marker of mineralisation, the effect of *RUNX2* mutation on the *ALP* activity of DFCs was first tested. We found that *ALP* activity of the CON-DFCs increased approximately 1.2- to 1.5-fold after osteogenic induction for 7 days or 14 days ($P < 0.05$) (Figure 4A and B). *ALP* activity was reduced 60%-80% by the *RUNX2* mutation compared to the normal control whether under osteogenic induction or not ($P < 0.05$) (Figure 4A and B). *ALP* staining showed that *ALP* expression in the CCD-DFCs was lower than that of the control in the basal condition, and the difference was much clearer after osteogenic induction (Figure 4C), showing a similar result with *ALP* activity. Alizarin red staining revealed that mineralised nodules in CCD-DFCs were obviously fewer than the normal control after osteogenic induction for 21 days (Figure 4D), indicating reduced mineralisation in CCD patients.
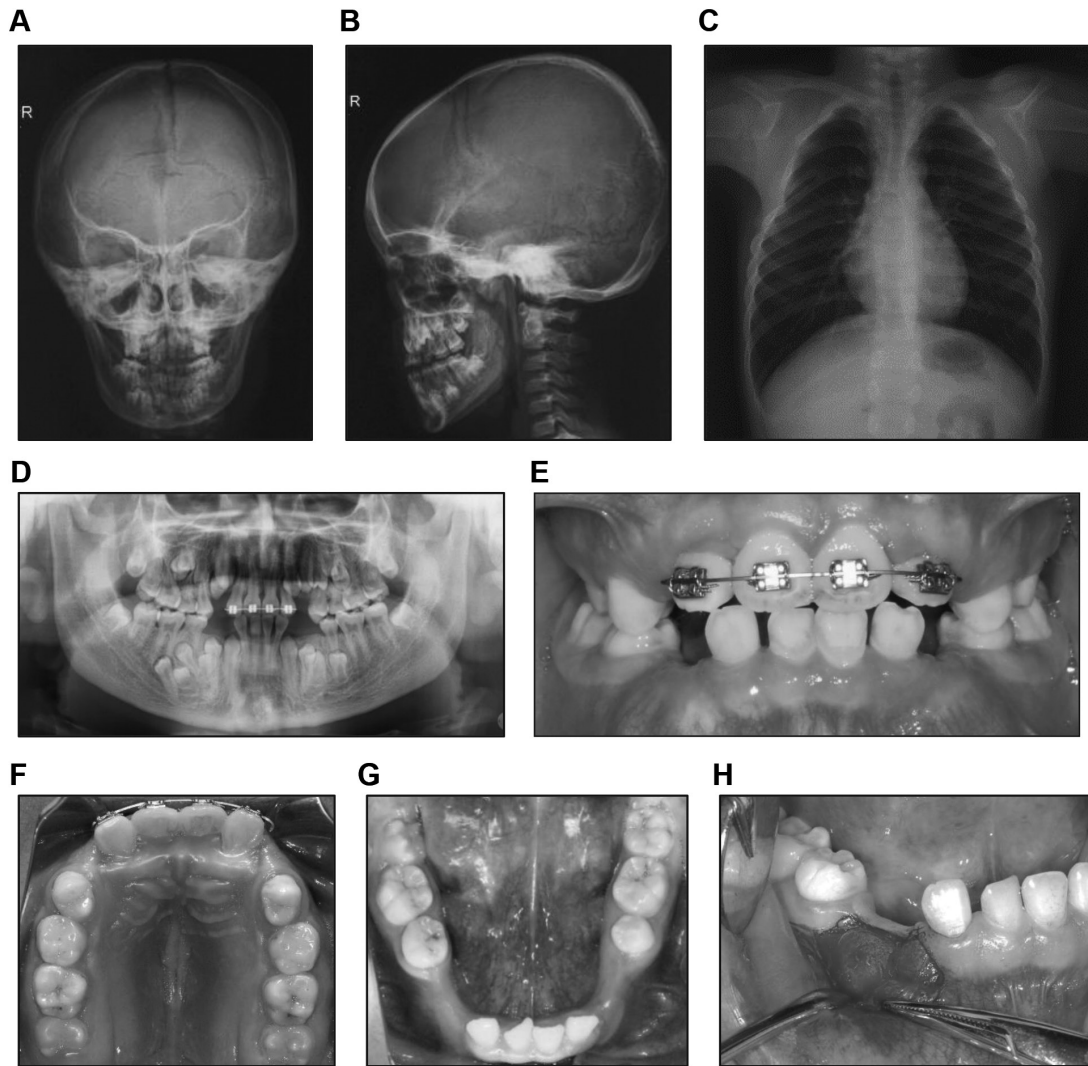
Figure 1. Clinical manifestation of the CCD patient. (A–D) Anteroposterior (A), lateral (B), Chest (C) and panoramic (D) radiograph of the CCD patient. (E–G) Intraoral photograph of the CCD patient. (H) Dental follicles of the impacted canine and premolar were surgically exposed.

The effect of *RUNX2* mutation on the expression of osteoblast-specific genes was thereafter evaluated. The mRNA level of RUNX2 in DFCs was decreased approximately 50% by the *RUNX2* mutation both in basal and osteogenic media found in the CCD group ($P < 0.05$) (Figure 4E). Consistently, the mRNA level of osteogenic markers, such as ALP, OSX, OCN and Col Iα1, was reduced 20–70% by the RUNX2 mutation ($P < 0.05$) (Figure 4F–I). Western blotting results indicated that the protein level of RUNX2, Col Iα1, ALP, OSX and OCN in CCD-DFCs was significantly decreased compared with the normal control in both basal and osteogenic media (Figure 4J).

Overexpression of *WT-RUNX2* restores the expression of *RUNX2* in DFCs from CCD patient

Our above-mentioned data showed that *RUNX2* mutation reduced *RUNX2* expression and interfered with the osteogenic ability of DFCs. To investigate whether recovering *RUNX2* expression in CCD-DFCs would rescue the osteogenic deficiency of DFCs caused by *RUNX2* mutation, we constructed lentivirus that expresses full-length *WT-RUNX2* with a GFP tag and infected CCD-DFCs. A lentivirus carrying a GFP tag without the target gene was used as

control. The results showed that GFP expression was observed in more than 90% of the stably infected DFCs under fluorescent microscopy in all groups (Figure 5A). *RUNX2* mRNA level was increased 5-fold in CCD DFCs stably infected with *WT-RUNX2* ($P < 0.05$) (Figure 5B). Consistently, western blot results showed that overexpression of *WT-RUNX2* in CCD-DFCs restored the reduced RUNX2 expression caused by *RUNX2* mutation (Figure 5C). These results indicated that the reduced *RUNX2* expression caused by *RUNX2* mutation was successfully rescued by infection of *WT-RUNX2* using lentivirus.

RUNX2 restoration rescues the reduced mineralisation of DFCs caused by *RUNX2* mutation

The effect of *RUNX2* restoration on the mineralised deficiency of DFCs caused by *RUNX2* mutation was investigated using the above-mentioned stably infected cells. *ALP* activity test revealed that *ALP* activity was decreased 70–90% by *RUNX2* mutation under basal or osteogenic conditions ($P < 0.05$) (Figure 6A and B). Overexpression of *WT-RUNX2* in CCD-DFCs resulted in a 1.5- to 7-fold increase in *ALP* activity compared to the CCD-DFCs infected
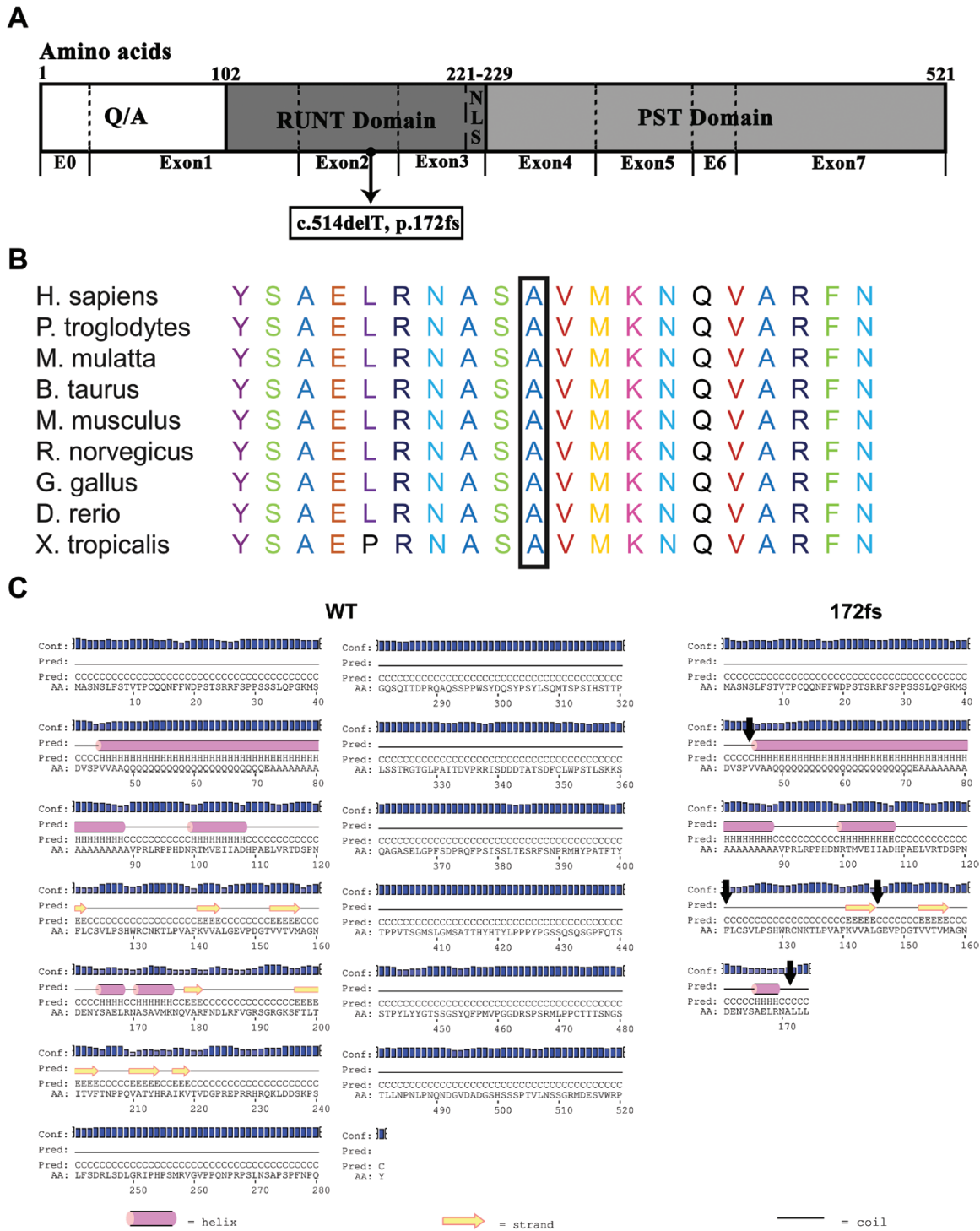
Figure 2. Mutation analysis of *RUNX2* gene for the CCD patient. (A) The location of *RUNX2* mutation in the CCD patient in the present study. Q/A, glutamine/alanine-rich region; RUNT, runt homology domain; NLS, nuclear-localisation signal; PST, proline/serine/threonine-rich region. (B) Conservation analysis of RUNX2, the positions of the mutated amino acid in our study are indicated using black boxes. (C) Secondary structure analysis of mutated RUNX2. Transformations are marked with black arrows. Pink cylinders represent the helix, yellow arrows represent the strand, and the straight line represents the coil.

with GFP control, whether under osteogenic induction or not ($P < 0.05$) (Figure 6A and B). Notably, *ALP* activity in CCD-DFCs infected with *WT-RUNX2* was almost increased to the level of the normal control after osteogenic induction for 14 days (Figure 6B). Similarly, *ALP* staining results showed a lower *ALP* expression in CCD-DFCs, while this reduction was

significantly rescued after infection of *WT-RUNX2*, especially under osteogenic condition (Figure 6C). Alizarin red staining results presented a similar trend as *ALP* staining that over-expression of *WT-RUNX2* noticeably rescued the decreased mineralised nodules in CCD-DFCs after osteogenic induction for 21 days (Figure 6D). These results indicated that
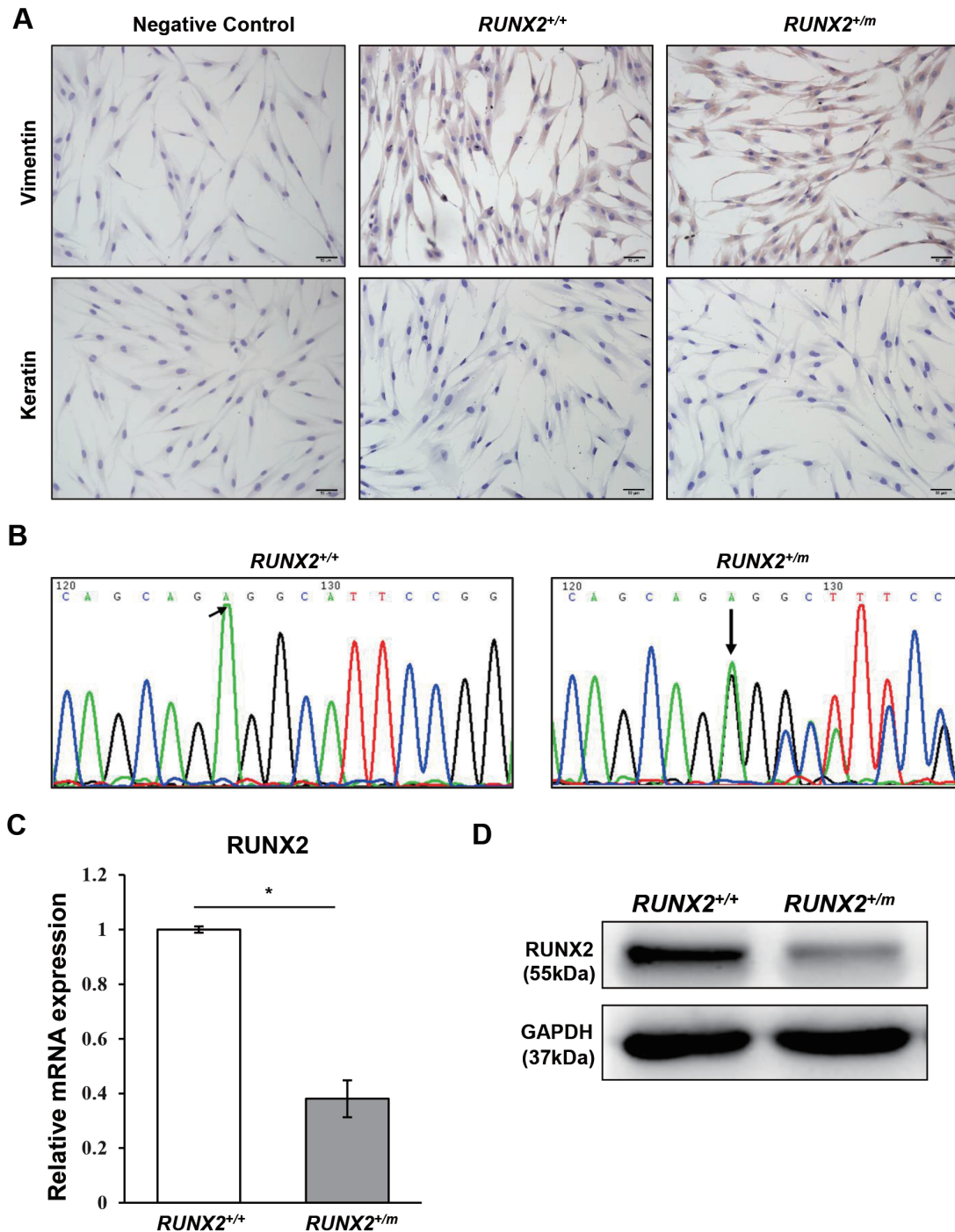
Figure 3. Biological characterisation of the DFCs from the CCD patient. Primary DFCs were isolated from the normal control (*RUNX2*+/+) and CCD patient (*RUNX2*+/m). (A) Immunohistochemistry staining of vimentin and keratin for DFCs. Scale bar, 50 μm. (B) Reverse sequencing data of *RUNX2* exon 2 from the CCD patient and normal control DFCs. Arrows indicate the mutation site. (C) Quantitative analysis of the mRNA level of *RUNX2* in DFCs. (D) Western-blot assay analysed the protein level of RUNX2 in DFCs. *$P < 0.05$.

overexpression of *WT-RUNX2* rescued the reduced mineralisation of CCD-DFCs.

RUNX2 restoration rescues the abnormal expression of osteoblast-associated genes caused by *RUNX2* mutation in DFCs

The effect of *RUNX2* restoration on the expression of osteoblast-associated genes was further explored using stably transfected cells.

RUNX2 mRNA level was reduced 20–40% by *RUNX2* mutation in both basal and osteogenic conditions ($P < 0.05$) (Figure 7A), which was consistent with the data shown in Figure 4. RUNX2 expression in CCD-DFCs was increased more than 4-fold by overexpression of *WT-RUNX2* whether under osteogenic induction or not ($P < 0.05$) (Figure 7A). Consistently, the expression of osteogenic markers, such as ALP, OSX, OCN and Col Iα1, was increased 1.3- to 3.5-fold by overexpression of *WT-RUNX2* in CCD-DFCs
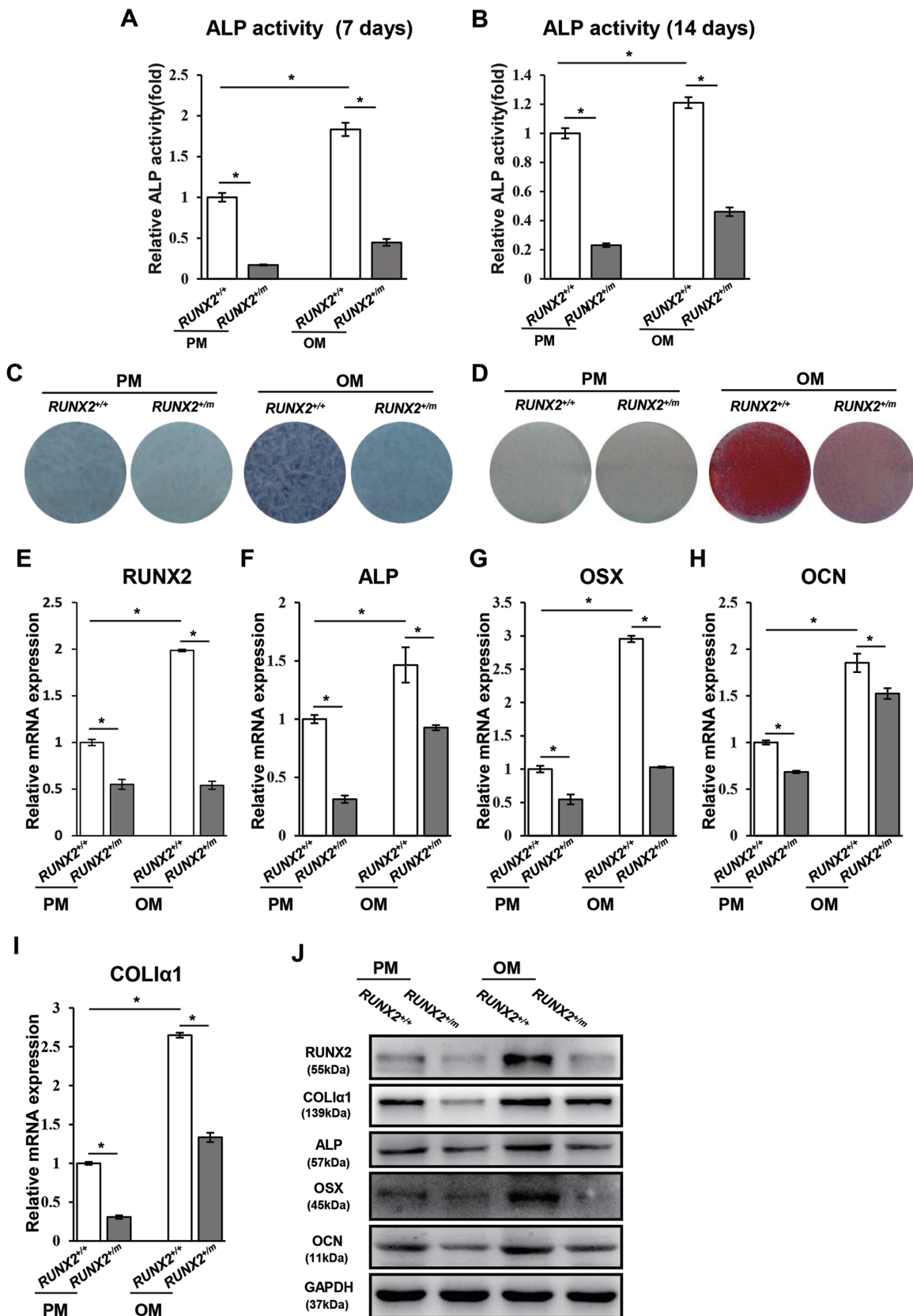
Figure 4. *RUNX2* mutation interfered with the osteogenic ability of primary DFCs. DFCs from the normal control (*RUNX2*+/+) and CCD patient (*RUNX2*+/m) were cultured in PM or OM. (A and B) *ALP* activity of DFCs was analysed after incubation in PM or OM for 7 days (A) or 14 days (B). (C) *ALP* staining of DFCs after induction in PM or OM for 14 days. (D) Alizarin red staining of mineralised nodules for DFCs after induction in PM or OM for 21 days. (E–I) Quantitative analysis of the mRNA levels of *RUNX2, ALP, OSX, OCN* and *COLα1* in DFCs after the cells were cultured in PM or OM for14 days. (J) Western-blot assay analysed the protein level of RUNX2, Col Iα1, ALP, OSX and OCN in DFCs after the cells were cultured in PM or OM for 14 days. *P < 0.05.
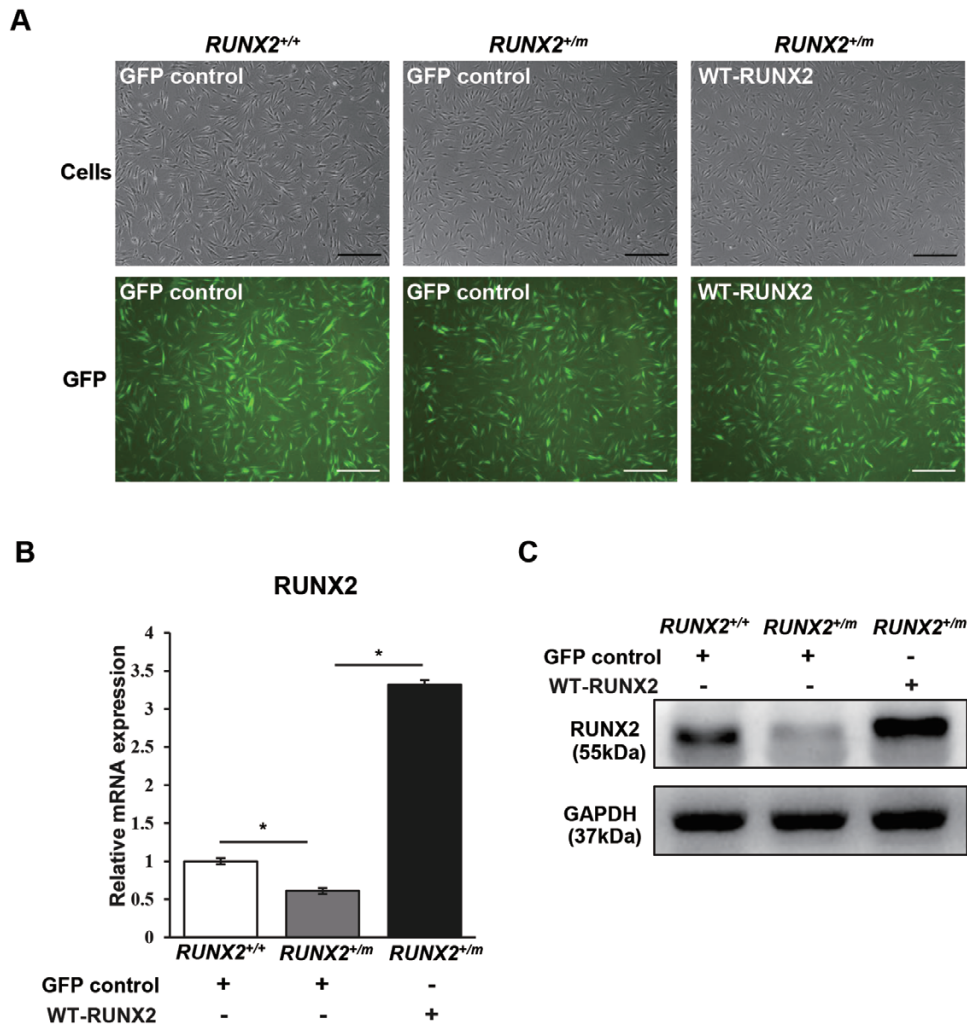
Figure 5. Overexpression of *WT-RUNX2* restored the expression of *RUNX2* in DFCs from the CCD patient. DFCs from the normal control (*RUNX2+/+*) or CCD patient (*RUNX2+/m*) were stably infected with the lentivirus of GFP control or *WT-RUNX2*. (A) GFP expression in DFCs after the cells were infected with the lentivirus of GFP control or *WT-RUNX2*. Scale bar, 500 μm. (B) Quantitative analysis of the mRNA level of *RUNX2* in stably infected DFCs. (C) Western-blot assay examined the protein level of RUNX2 in stably infected DFCs. *$P < 0.05$.

after osteogenic induction for 14 days ($P < 0.05$) (Figure 7B–E), indicating the induction effect of *RUNX2* on the expression of the above-mentioned genes.

Western blotting results indicated that the protein level of RUNX2 was reduced in CCD-DFCs compared to CON-DFCs (Figure 7F). And a similar pattern was found in the protein level of Col Iα1, ALP, OSX and OCN when *RUNX2* was abnormal. Consistently, overexpression of *WT-RUNX2* apparently increased the protein level of RUNX2, Col Iα1, ALP, OSX and OCN, especially under osteogenic condition (Figure 7F), indicating the rescue effect of *RUNX2* restoration on the expression of these key osteoblast-associated genes.

Discussion

In this study we presented a CCD patient with typical CCD features, including delayed eruption of permanent teeth. The *RUNX2* heterozygous mutation (c.514delT, p.172fs) found in the CCD patient interfered with the osteogenic capacity and expression of osteoblast-specific genes in DFCs. Restoration of *RUNX2* in CCD-DFCs partially rescued the mineralised deficiency of CCD-DFCs. The abnormal

expression of osteoblast-associated genes caused by *RUNX2* mutation was also restored by overexpression of *WT-RUNX2* both at mRNA and protein level. All the results illustrated that *RUNX2* mutation reduced osteogenic capacity of DFCs through inhibiting osteoblast-associated genes, therefore interfering with bone formation and the motive force for tooth eruption.

The RUNT domain of RUNX2 protein is a characteristic and highly conserved motif, which is mainly responsible for DNA-binding to the promoters of its downstream target genes and heterodimerisation with core binding factor β (CBFβ) (27). Though CBFβ does not bind DNA directly, it enhances the DNA binding capacity of RUNX2 protein. The *RUNX2* mutation found in the present CCD patient is located in the RUNT domain, and the conservation analysis showed that the affected residues are highly conserved among different species, indicating this mutation may disturb the binding ability of RUNX2. It has been revealed that protein structure is a decisive factor for its function, and transformation of protein structure may lead to destruction of the protein function (28). The secondary structural analysis showed that the 172fs mutation altered the RUNT domain secondary structure of RUNX2 protein, indicating that this mutation may affect the heterodimerisation
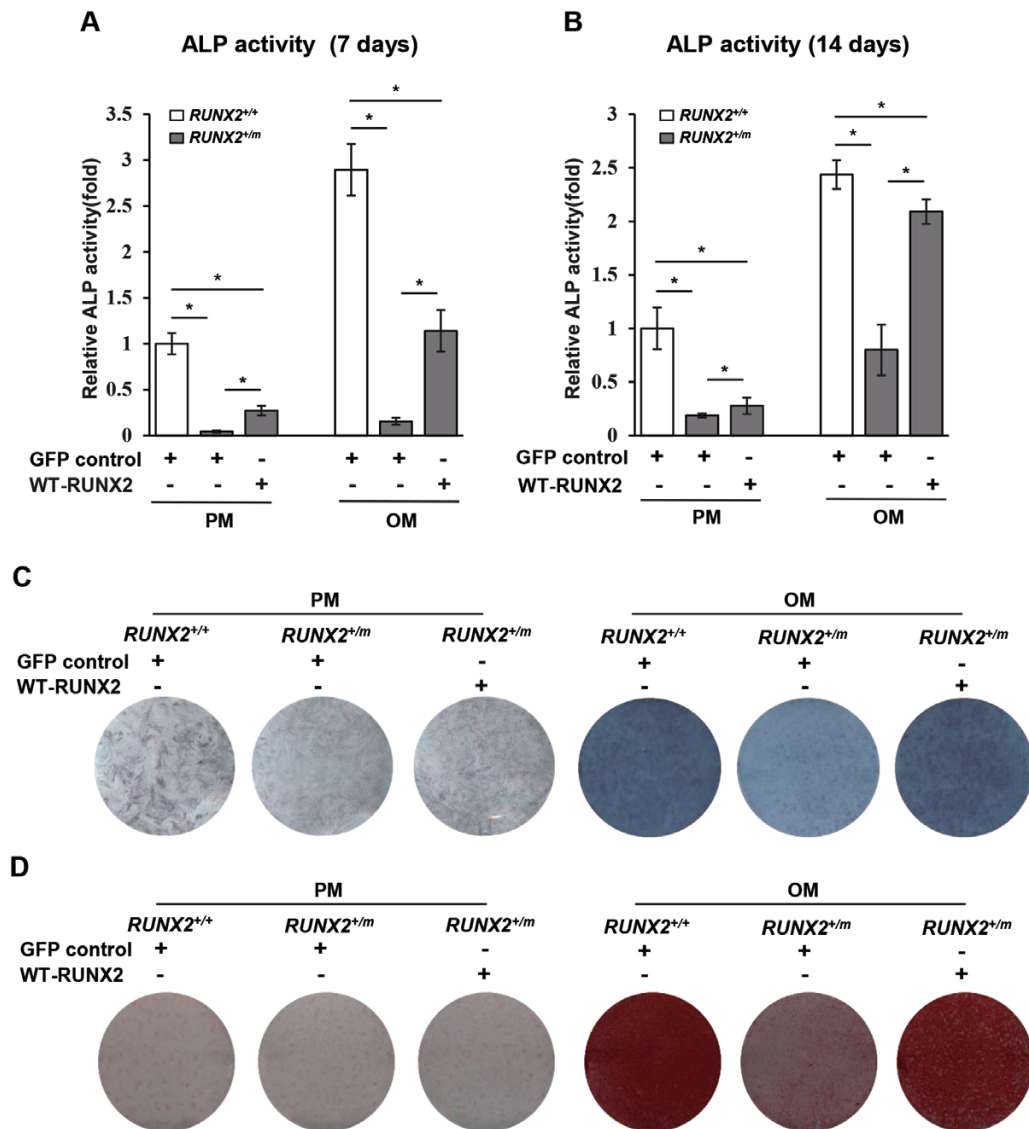
Figure 6. *RUNX2* restoration rescued the reduced mineralisation of DFCs caused by *RUNX2* mutation. DFCs from the normal control (*RUNX2$^{+/+}$*) or CCD patient (*RUNX2$^{+/m}$*) were infected with the lentivirus of GFP control or *WT-RUNX2*, and then the cells were cultured in PM or OM. (A and B) *ALP* activity of DFCs was analysed after incubation in PM or OM for 7 days (A) or 14 days (B). (C) *ALP* staining of DFCs after induction in PM or OM for 14 days. (D) Alizarin red staining of mineralised nodules for DFCs after induction in PM or OM for 21 days. *$P < 0.05$.

activity between RUNX2 and CBFβ and impair subsequent DNA binding and transactivation ability.

RUNX2 is known for its diversified function in different tissues. *RUNX2* has been reported to be constitutively expressed in differentiated DFCs whether under osteogenic induction or not (29,30). In the present study, we found that *RUNX2* expression in DFCs was decreased by the *RUNX2* mutation found in the CCD patient. This can be explained that the frameshift mutation found in the CCD patient produced a premature protein truncated at the RUNT domain with only 174 amino acid residues, and the truncated proteins may be unstable and can be degraded rapidly (31). We also found that the expression of osteoblast-related genes, including *ALP*, *OCN* and *Col Iα1* was reduced compared to the normal control when *RUNX2* mutation was present in DFCs. This was because the osteoblast-specific element 2 (OSE2), the core binding factor site of RUNX2 protein, was present in the promoter region of the above-mentioned osteoblast-specific genes (32). And *RUNX2* mutation can significantly reduce

the transactivation ability of RUNX2 on OSE2 (15,33). Therefore, it can be speculated that *RUNX2* mutation found in the CCD patient reduced the mineralisation capacity of DFCs by downregulating its downstream osteogenic associated genes directly.

Tooth eruption is a localised event that requires chronologically and spatially specific bone remodelling regulated by the dental follicle that surrounds the unerupted tooth (19). Alveolar bone resorption at the coronal area of tooth bulb is indispensable for the formation of tooth eruption pathway, and the tooth can move through this pathway. Many studies have shown that alveolar bone growth at the base of the crypt serves as the major motive force to propel the tooth through its eruption pathway (20,34,35). Scanning electron microscopy (SEM) studies demonstrated active bone formation at the base of the crypt in the erupting mandibular molars of rats (36). It has been determined that DFCs exhibit pluripotency in being able to differentiate to alveolar osteoblasts and participate in bone formation during tooth eruption (20,23,24). Previous studies showed that if bone formation was blocked in the local
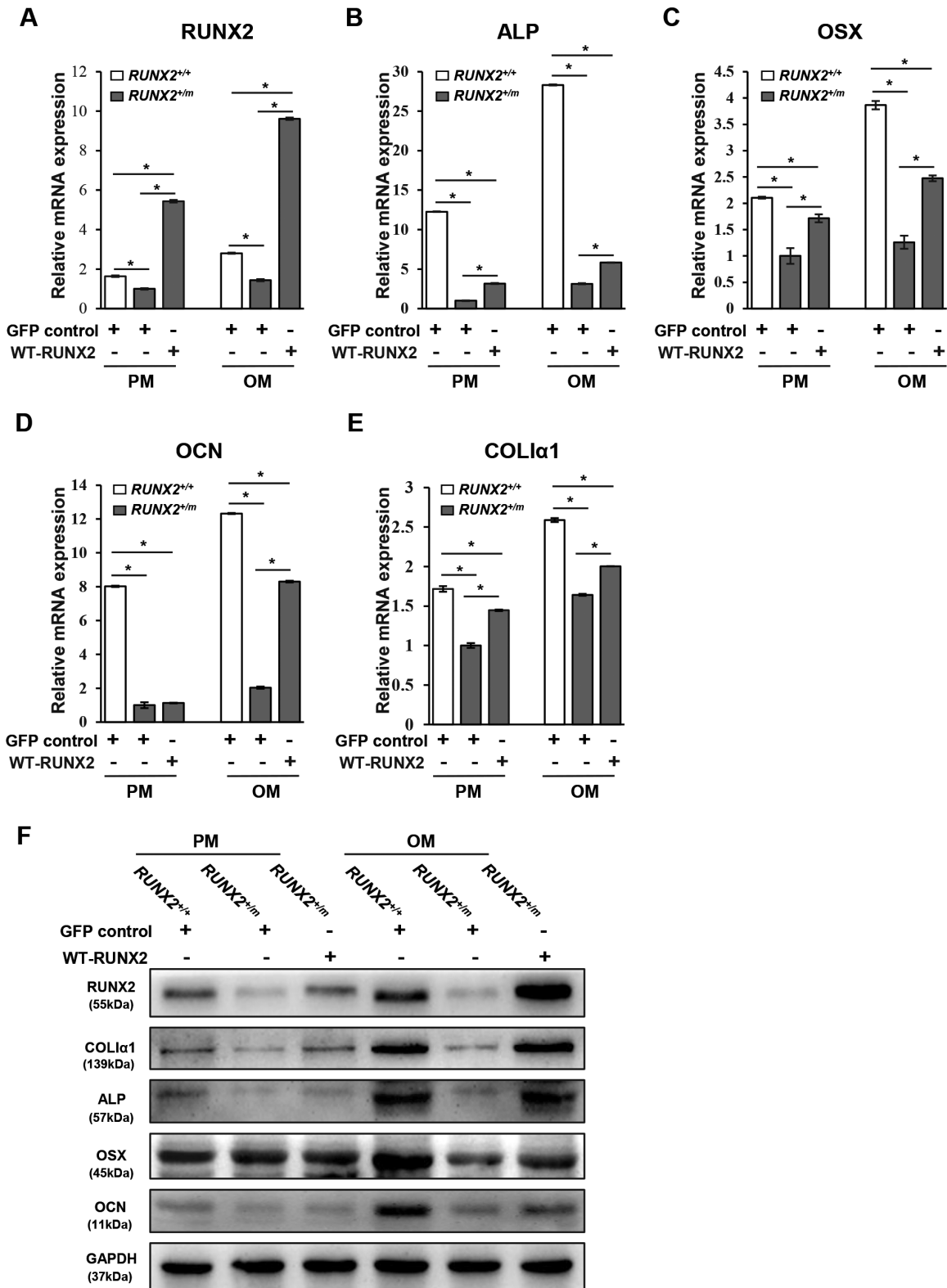
Figure 7. *RUNX2* restoration rescued the abnormal expression of osteoblast-associated genes caused by *RUNX2* mutation in DFCs. DFCs from the normal control (*RUNX2⁺/⁺*) or CCD patient (*RUNX2⁺/ᵐ*) were infected with the lentivirus of GFP control or *WT-RUNX2*, and then the cells were cultured in PM or OM. (A–E) Quantitative analysis of the mRNA levels of *RUNX2*, *ALP*, *OSX*, *OCN* and *COLIα1* in DFCs after the cells were cultured in PM or OM for 14 days. (F) Western-blot assay analysed the protein level of *RUNX2*, *COLIα1*, *ALP*, *OSX* and *OCN* in DFCs after the cells were cultured in PM or OM for 14 days. *$P < 0.05$.

region, an eruption pathway was normally formed but the tooth was still impacted for a lack of eruption force (35,37,38). Based on these studies, our data showed that *RUNX2* mutation significantly decreased

the mineralisation ability of CCD-DFCs, which may lead to the deficiency of motive force for the unerupted tooth, causing delayed permanent tooth eruption in CCD patients.

To investigate whether the osteogenic deficiency of CCD-DFCs can be rescued by restoration of *RUNX2* expression, we performed 'rescue' experiments. Our result showed that recovery of *RUNX2* expression in CCD-DFCs restored the mineralised deficiency and the abnormal expression of *RUNX2* downstream molecules, such as *ALP*, *OSX*, *OCN* and *Col Iα1*. This is in accordance with a previous study which reported that *RUNX2* plays critical roles in the osteogenic differentiation of DFCs by regulating expression of osteogenic markers (23). Overexpression of *RUNX2* in DFCs could increase the expression levels of OPN, Col I, OCN and BSP, and enhance the mineralisation of DFCs (23). These findings provided sufficient evidence for the fact that *RUNX2* mutation is the cause of the reduced osteogenic differentiation of CCD-DFCs and indicated that *RUNX2* is essential for alveolar bone growth during tooth eruption. Our data also inspired that *RUNX2* is likely to be a target gene for therapy of delayed permanent tooth eruption in CCD patients.

In summary, this study suggests that *RUNX2* mutation inhibits the expression of osteoblast-specific genes in DFCs, such as *RUNX2*, *ALP*, *OSX*, *OCN* and *Col Iα1*, thereafter interfering with osteogenic capacity of DFCs. This effect restricts alveolar bone formation at the base of tooth crypt, which serves as an eruption force to propel the tooth out of its bony crypt. Our findings provide valuable explanations and implications for the mechanism of delayed permanent tooth eruption in CCD patients.

References

1. Komori, T., Yagi, H., Nomura, S., *et al.* (1997) Targeted disruption of Cbfa1 results in a complete lack of bone formation owing to maturational arrest of osteoblasts. *Cell*, 89, 755–764.
2. Otto, F., Thornell, A. P., Crompton, T., *et al.* (1997) Cbfa1, a candidate gene for cleidocranial dysplasia syndrome, is essential for osteoblast differentiation and bone development. *Cell*, 89, 765–771.
3. Komori, T. (2017) Roles of Runx2 in skeletal development. *Adv. Exp. Med. Biol.*, 962, 83–93.
4. Zhao, W., Zhang, S., Wang, B., Huang, J., Lu, W. W. and Chen, D. (2016) Runx2 and microRNA regulation in bone and cartilage diseases. *Ann. N. Y. Acad. Sci.*, 1383, 80–87.
5. Bruderer, M., Richards, R. G., Alini, M. and Stoddart, M. J. (2014) Role and regulation of RUNX2 in osteogenesis. *Eur. Cell. Mater.*, 28, 269–286.
6. Hecht, J., Seitz, V., Urban, M., *et al.* (2007) Detection of novel skeletogenesis target genes by comprehensive analysis of a Runx2(-/-) mouse model. *Gene Expr. Patterns*, 7, 102–112.
7. Nakashima, K., Zhou, X., Kunkel, G., Zhang, Z., Deng, J. M., Behringer, R. R. and de Crombrugghe, B. (2002) The novel zinc finger-containing transcription factor osterix is required for osteoblast differentiation and bone formation. *Cell*, 108, 17–29.
8. Ducy, P., Zhang, R., Geoffroy, V., Ridall, A. L. and Karsenty, G. (1997) Osf2/Cbfa1: a transcriptional activator of osteoblast differentiation. *Cell*, 89, 747–754.
9. Javed, A., Barnes, G. L., Jasanya, B. O., Stein, J. L., Gerstenfeld, L., Lian, J. B. and Stein, G. S. (2001) Runt homology domain transcription factors (Runx, Cbfa, and AML) mediate repression of the bone sialoprotein promoter: evidence for promoter context-dependent activity of Cbfa proteins. *Mol. Cell. Biol.*, 21, 2891–2905.
10. Sato, M., Morii, E., Komori, T., *et al.* (1998) Transcriptional regulation of osteopontin gene in vivo by PEBP2alphaA/CBFA1 and ETS1 in the skeletal tissues. *Oncogene*, 17, 1517–1525.
11. Zaidi, S. K., Javed, A., Choi, J. Y., van Wijnen, A. J., Stein, J. L., Lian, J. B. and Stein, G. S. (2001) A specific targeting signal directs Runx2/Cbfa1 to subnuclear domains and contributes to transactivation of the osteocalcin gene. *J. Cell Sci.*, 114, 3093–3102.
12. Lee, B., Thirunavukkarasu, K., Zhou, L., Pastore, L., Baldini, A., Hecht, J., Geoffroy, V., Ducy, P. and Karsenty, G. (1997) Missense mutations abolishing DNA binding of the osteoblast-specific transcription factor OSF2/CBFA1 in cleidocranial dysplasia. *Nat. Genet.*, 16, 307–310.
13. Mundlos, S. (1999) Cleidocranial dysplasia: clinical and molecular genetics. *J. Med. Genet.*, 36, 177–182.
14. Quack, I., Vonderstrass, B., Stock, M., *et al.* (1999) Mutation analysis of core binding factor A1 in patients with cleidocranial dysplasia. *Am. J. Hum. Genet.*, 65, 1268–1278.
15. Zhang, C. Y., Zheng, S. G., Wang, Y. X., Zhu, J. X., Zhu, X., Zhao, Y. M. and Ge, L. H. (2009) Novel RUNX2 mutations in Chinese individuals with cleidocranial dysplasia. *J. Dent. Res.*, 88, 861–866.
16. Zhang, C., Zheng, S., Wang, Y., Zhao, Y., Zhu, J. and Ge, L. (2010) Mutational analysis of RUNX2 gene in Chinese patients with cleidocranial dysplasia. *Mutagenesis*, 25, 589–594.
17. Jensen, B. L. and Kreiborg, S. (1990) Development of the dentition in cleidocranial dysplasia. *J. Oral Pathol. Med.*, 19, 89–93.
18. Proffit, W. R. and Frazier-Bowers, S. A. (2009) Mechanism and control of tooth eruption: overview and clinical implications. *Orthod. Craniofac. Res.*, 12, 59–66.
19. Wise, G. E. (2009) Cellular and molecular basis of tooth eruption. *Orthod. Craniofac. Res.*, 12, 67–73.
20. Wise, G. E. and King, G. J. (2008) Mechanisms of tooth eruption and orthodontic tooth movement. *J. Dent. Res.*, 87, 414–434.
21. Liu, D. and Wise, G. E. (2007) A DNA microarray analysis of chemokine and receptor genes in the rat dental follicle–role of secreted frizzled-related protein-1 in osteoclastogenesis. *Bone*, 41, 266–272.
22. Yao, S., Li, C., Beckley, M. and Liu, D. (2017) Expression of odontogenic ameloblast-associated protein in the dental follicle and its role in osteogenic differentiation of dental follicle stem cells. *Arch. Oral Biol.*, 78, 6–12.
23. Pan, K., Sun, Q., Zhang, J., Ge, S., Li, S., Zhao, Y. and Yang, P. (2010) Multilineage differentiation of dental follicle cells and the roles of Runx2 over-expression in enhancing osteoblast/cementoblast-related gene expression in dental follicle cells. *Cell Prolif.*, 43, 219–228.
24. Saugspier, M., Felthaus, O., Viale-Bouroncle, S., Driemel, O., Reichert, T. E., Schmalz, G. and Morsczeck, C. (2010) The differentiation and gene expression profile of human dental follicle cells. *Stem Cells Dev.*, 19, 707–717.
25. Wang, X. Z., Sun, X. Y., Zhang, C. Y., Yang, X., Yan, W. J., Ge, L. H. and Zheng, S. G. (2016) RUNX2 mutation impairs 1α,25-Dihydroxyvitamin D3 mediated osteoclastogenesis in dental follicle cells. *Sci. Rep.*, 6, 24225.
26. Yan, W. J., Zhang, C. Y., Yang, X., Liu, Z. N., Wang, X. Z., Sun, X. Y., Wang, Y. X. and Zheng, S. G. (2015) Abnormal differentiation of dental pulp cells in cleidocranial dysplasia. *J. Dent. Res.*, 94, 577–583.
27. Tahirov, T. H., Inoue-Bungo, T., Morii, H., *et al.* (2001) Structural analyses of DNA recognition by the AML1/Runx-1 Runt domain and its allosteric control by CBFbeta. *Cell*, 104, 755–767.
28. Han, M. S., Kim, H. J., Wee, H. J., *et al.* (2010) The cleidocranial dysplasia-related R131G mutation in the Runt-related transcription factor RUNX2 disrupts binding to DNA but not CBF-beta. *J. Cell. Biochem.*, 110, 97–103.
29. Morscczeck, C. (2006) Gene expression of runx2, Osterix, c-fos, DLX-3, DLX-5, and MSX-2 in dental follicle cells during osteogenic differentiation in vitro. *Calcif. Tissue Int.*, 78, 98–102.

30. Morsczeck, C., Schmalz, G., Reichert, T. E., Völlner, F., Saugspier, M., Viale-Bouroncle, S. and Driemel, O. (2009) Gene expression profiles of dental follicle cells before and after osteogenic differentiation in vitro. *Clin. Oral Investig.*, 13, 383–391.

31. Xuan, D., Sun, X., Yan, Y., Xie, B., Xu, P. and Zhang, J. (2010) Effect of cleidocranial dysplasia-related novel mutation of RUNX2 on characteristics of dental pulp cells and tooth development. *J. Cell. Biochem.*, 111, 1473–1481.

32. Ducy, P. (2000) Cbfa1: a molecular switch in osteoblast biology. *Dev. Dyn.*, 219, 461–471.

33. Zhang, X., Liu, Y., Wang, X., Sun, X., Zhang, C. and Zheng, S. (2017) Analysis of novel RUNX2 mutations in Chinese patients with cleidocranial dysplasia. *PLoS One*, 12, e0181653.

34. Wise, G. E., He, H., Gutierrez, D. L., Ring, S. and Yao, S. (2011) Requirement of alveolar bone formation for eruption of rat molars. *Eur. J. Oral Sci.*, 119, 333–338.

35. Xu, H., Snider, T. N., Wimer, H. F., Yamada, S. S., Yang, T., Holmbeck, K. and Foster, B. L. (2016) Multiple essential MT1-MMP functions in tooth root formation, dentinogenesis, and tooth eruption. *Matrix Biol.*, 52-54, 266–283.

36. Wise, G. E., Yao, S. and Henk, W. G. (2007) Bone formation as a potential motive force of tooth eruption in the rat molar. *Clin. Anat.*, 20, 632–639.

37. Bartlett, J. D., Zhou, Z., Skobe, Z., Dobeck, J. M. and Tryggvason, K. (2003) Delayed tooth eruption in membrane type-1 matrix metalloproteinase deficient mice. *Connect. Tissue Res.*, 44 (Suppl 1), 300–304.

38. Beertsen, W., Holmbeck, K., Niehof, A., Bianco, P., Chrysovergis, K., Birkedal-Hansen, H. and Everts, V. (2002) On the role of MT1-MMP, a matrix metalloproteinase essential to collagen remodeling, in murine molar eruption and root growth. *Eur. J. Oral Sci.*, 110, 445–451.